

SCANNING-PROTON-MICROPROBE MAPPING OF MINOR AND TRACE ELEMENTS ALONG MINERAL CLEAVAGES, FRACTURES AND GRAIN BOUNDARIES: EVIDENCE FOR ELEMENT MOBILITY

NORMAN M. HALDEN

Department of Geological Sciences, University of Manitoba, Winnipeg, Manitoba R3T 2N2

WILLIAM J. TEESDALE AND JOHN L. CAMPBELL

Guelph-Waterloo Program for Graduate Work in Physics, University of Guelph, Guelph, Ontario N1G 2W1

ABSTRACT

The scanning proton-microprobe and proton-induced X-ray emission have been used to map and analyze the distribution of trace elements at grain boundaries, fractures and cleavage planes in a rare-element-enriched pegmatitic syenite from the Eden Lake syenite complex, Manitoba. In the vicinity of metamict britholite, fractures and cleavages in minerals and grain boundaries between minerals show elevated abundances of rare earth, alkali, transition and large-ion lithophile elements. The elements were probably released from metamict britholite and deposited from a fluid that had migrated along these surfaces after the crystallization of the rock. Semiquantitative point analyses were done on fractures in quartz and K-feldspar cleavages, where problems related to matrix corrections are minimized. These features show local concentrations of *ca.* 200 ppm Mn, 4500 ppm Fe, 30 ppm Zn, 10 ppm Rb, 100 ppm Sr, 100 ppm Y, 200–700 ppm Nd, 20–50 ppm Pb, 30 ppm Th and 70 ppm U. These levels are significantly higher than what is found in the surrounding undamaged quartz and between cleavages in K-feldspar.

Keywords: proton-induced X-ray emission, μ -PIXE, scanning proton microprobe, trace elements, element mobility.

SOMMAIRE

Nous nous sommes servi d'une microsonde protonique à balayage et d'une analyse d'émissions de rayons X induites par faisceau de protons pour évaluer la répartition des éléments traces le long des bordures, des fractures et des clivages des cristaux d'une pegmatite syénitique enrichie en éléments exotiques du complexe syénitique de Eden Lake, au Manitoba. Tout près des cristaux de britholite (métamictite), les fractures, les clivages et les bordures des minéraux font preuve d'une augmentation en teneurs des terres rares, alcalins, éléments de transition et éléments lithophiles à large rayon. Ces éléments auraient été lessivés de la britholite et déposés à partir d'une phase fluide migrant le long de ces surfaces une fois la roche cristallisée. Nous avons effectué des analyses ponctuelles semi-quantitatives le long des fractures dans le quartz et des clivages dans le feldspath alcalin, où les corrections dues aux effets de matrice sont aptes à être minimales. Nous avons trouvé des concentrations locales de l'ordre de 200 ppm de Mn, 4500 ppm de Fe, 30 ppm de Zn, 10 ppm de Rb, 100 ppm de Sr et d'Y, de 200 à 700 ppm de Nd, de 20 à 50 ppm de Pb, 30 ppm de Th et 70 ppm d'U. Ces niveaux de concentration dépassent de beaucoup ceux qui caractérisent le quartz non endommagé et les clivages d'un cristal de feldspath alcalin moins affecté.

(Traduit par la Rédaction)

Mots-clés: émissions de rayons X induites par faisceau de protons, micro-PIXE, microsonde protonique à balayage, éléments traces, mobilité des éléments.

INTRODUCTION

The distribution of elements within and between minerals reflects the physical and chemical characteristics of (i) the environment in which minerals crystallize, and (ii) the conditions of any later recrystallization or alteration event. The environment, commonly defined in terms of pressure, temperature and bulk chemistry, may change with time, in response

to which a mineral may alter its structure and composition. Alteration is usually attributed to reaction with a chemically reactive fluid, and is likely to occur initially at the surface of the mineral (*cf.* Hochella & White 1990). In general, in real geological situations, the chemically reactive fluid phase has been lost, and we are left with only a partial record of the processes involved and of the chemistry of the fluid. Fluid inclusions may retain a record of the chemistry of the

fluid, but they are difficult to analyze and usually variable in their composition; furthermore, owing to analytical limitations, emphasis is usually placed on understanding their major-element chemistry (*cf.* Anderson *et al.* 1989). To determine the abundance of trace elements requires a technique with sufficient sensitivity and excellent spatial resolution on a micrometer scale.

In the case of igneous rocks, it is often assumed that once the minerals have crystallized, the elements they host remain, on the whole, immobile. Of particular interest from a petrogenetic point of view are the High Field-Strength Elements (*HFSE*) Ta, Hf, Zr and Y, the Rare-Earth Elements (*REE*); and the Large-Ion Lithophile Elements (*LILE*) U, Pb and Th. Many tectonic discriminant diagrams and petrogenetic models hinge on the idea that such elements are immobile during alteration and even weathering. However, Goni (1966) showed, using selective acid leaching on granitic rocks, that significant concentrations of trace elements were to be found weakly adhered to mineral surfaces and on mineral cleavages and fracture surfaces. Despite this, it is common, particularly in whole-rock analysis, to ignore the variations that can occur in the distribution of trace elements within and between minerals, especially that fraction that may be adhering to mineral surfaces.

Analytical strategies are often aimed at avoiding inhomogeneities and potential contamination; this usually stems from the inherent technical limitations of the analytical techniques used. The electron microprobe, while offering excellent spatial resolution, is usually restricted to the analysis of minerals for major and minor elements; inhomogeneities are routinely avoided because of problems connected with large excitation-volumes and effects due to secondary fluorescence.

Recent work done using Secondary-Ion Mass Spectrometry (SIMS), Laser-Ablation – Inductively Coupled Plasma – Mass Spectrometry (LA-ICP-MS; Jackson *et al.* 1992) and Proton-Induced X-ray Emission (PIXE; Fraser *et al.* 1984, Green *et al.* 1989, O'Reilly *et al.* 1991, Halden *et al.* 1993) has shown that we can now analyze samples for trace elements with good sensitivity and with spatial resolution on a scale of micrometers. A variant of PIXE, the Scanning Proton Microprobe (SPM), can be routinely used to map the distribution of trace elements in the form of two-dimensional X-ray maps or as line-scans (Fraser *et al.* 1984, Teesdale *et al.* 1993). Both can be used (at appropriate scales) to image the distribution of elements within minerals and a variety of other mineralogical features, such as grain boundaries and inclusions. In this study, we have used SPM and μ -PIXE to map the distribution of trace elements in fractures, grain boundaries and mineral cleavages from a rare-element-enriched syenite located at Eden Lake, central Manitoba.

SAMPLE DESCRIPTION, PREPARATION AND EXPERIMENTAL METHOD

The Eden Lake syenite is a coarse-grained rock consisting of pink-orange K-feldspar, aegirine-augite, blue-green amphibole and titanite, with accessory apatite, weloganite $[\text{Na}_2\text{Sr}_3\text{Zr}(\text{CO}_3)_6\cdot 3\text{H}_2\text{O}]$ and zircon (McRitchie 1988, Halden & Fryer, unpubl. data). Pegmatite bodies associated with the syenite can be subdivided into two broad groups, granitic pegmatites, which occur as irregular segregations within the main body of the syenite, and late cross-cutting pegmatites that contain significant concentrations of britholite $(\text{Ca}, \text{REE}, \text{Y})_5(\text{SiO}_4)_3(\text{PO}_4)_3(\text{F}, \text{OH})$. Titanite, zircon and apatite also are common in the pegmatites, but tend to be larger (*ca.* 5 mm in length) and euhedral. Zircon, apatite and titanite also show a similar history of crystallization in that they typically have a mottled core-region separated from an overgrowth showing oscillatory zoning by an irregular surface that would suggest a period of partial resorption in the magma. In the pegmatites, zircon and britholite are commonly metamict and surrounded by radial fractures, suggesting that metamictization has been accompanied by a volume change around these minerals.

In general, the syenite is significantly enriched in light rare-earth elements (*LREE*), U and Th. Compositional variation in the complex has been strongly influenced by crystal fractionation of the assemblage of primary minerals, consisting of K-feldspar, aegirine, titanite, zircon and apatite. This has resulted in elevated ΣREE contents in the more primitive magmas, with later silica-rich differentiates having lower ΣREE contents. The associated pegmatites have very high ΣREE contents and extremely *LREE*-enriched signatures (McRitchie 1989). Fluorite is very common in the pegmatitic phases; it has been suggested that segregation of a F-enriched vapor phase into the pegmatites, late in the evolution of the complex, has contributed to their extreme enrichment in *REE* (Halden & Fryer, unpubl. data).

Samples were prepared as carbon-coated polished thin sections ($\sim 50 \mu\text{m}$ thick). Areas to be scanned and analyzed using SPM and μ -PIXE were first imaged using Back-Scattered Electrons (BSE) and reflected light microscopy; BSE images and photomicrographs proved invaluable in locating minerals and correlating physical features with the X-ray maps.

The PIXE work was done on the Guelph Scanning Proton Microprobe (GSPM). A $5 \times 5 \mu\text{m}$ spot size with 3 MeV protons and an average beam-current of approximately 0.1 nA was used for point analyses; the resulting X-ray spectra were recorded with a Si(Li) detector. The time-integrated charge for each analysis was 2 μC . Spectra were processed using the Guelph PIXE software package GUPIX (Maxwell *et al.* 1989). A 3-MeV proton beam focussed to 5 μm by a small

air-cooled QL-300 magnetic quadrupole doublet also was used for the scanning work. For two-dimensional X-ray maps, the beam can be moved over a $250\ \mu\text{m} \times 250\ \mu\text{m}$ area on the specimen surface by two pairs of electrostatic plates located between the quadrupole focussing doublet and the specimen.

RESULTS

Figure 1 shows a BSE image of a zoned, lozenge-shaped crystal of titanite from the Eden Lake syenite, surrounded by quartz (black) and britholite (white); the variation in levels of grey corresponds to spatial variations in the average atomic number of the minerals. The britholite, a Ca-REE (Si,P) apatite analogue with elevated concentrations of Nd, U and Th (*i.e.*, it has a high average atomic number), tends to be white. On the other hand, quartz has a low average atomic number and appears black. The BSE image shows two characteristic features of such titanite grains: (i) the contact between titanite grains and quartz is defined by a thin white line, which would suggest the presence of a material with a high average atomic number, and (ii) there are numerous thin white lines cross-cutting the quartz adjacent to the titanite. The bright features cross-cutting the quartz correspond to the location of fractures in the quartz seen in transmitted and reflected light microscopy.

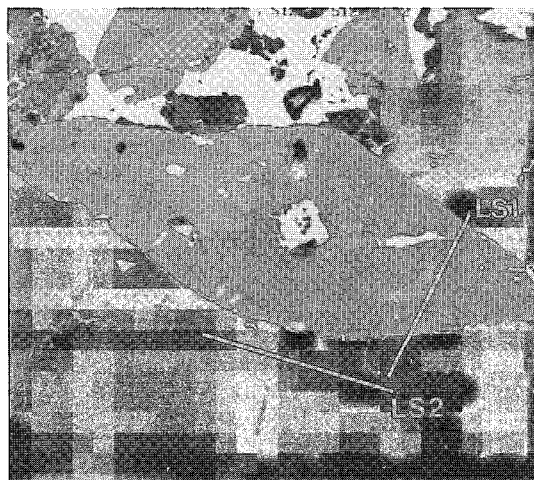


FIG. 1. BSE image of a titanite grain surrounded by quartz and metamict britholite; the field of view is $250\ \mu\text{m}$ wide. The white lines indicate the location of line scans LS1 and LS2 seen in Figures 3 and 4. The bright inclusion in the center of the titanite is weloganite.

Element maps and line-scans

Figure 2 is an SPM X-ray map of the titanite grain shown in Figure 1. The distribution and intensity of X rays (particularly those of Fe, Y, Sr and Nd) outline the lozenge shape of the titanite seen in the BSE image (Fig. 1). High concentrations of Sr and Nd show the position of a weloganite inclusion at the center of the titanite grain; the (total) X-ray spectrum also shows the presence of significant Zr. Table 1 shows the X-ray lines that were used to create the two-dimensional maps and line-scans. The principal problem with mapping the distribution of elements in this mineral assemblage is the abundance of Fe, particularly with regard to pile-up of Fe X-rays. To minimize the potential for overlap, the mapping window for each element of interest was severely restricted, in some cases to one tenth of the full width at half maximum (FWHM) of the X-ray line of interest (*ca.* 15 eV). Although this restriction reduces the number of X-ray events mapped, these are still sufficient to map the distribution of trace elements present at a level of a few tens of ppm. A second check for overlap problems involves a comparison of the distribution of the suspected overlapping element with that of the element of interest; a third check is derived from the point analyses. At this stage, peak overlaps are stripped from the spectrum as part of the spectrum-fitting process (Maxwell *et al.* 1989).

Elevated concentrations of Fe, Zn, Y and possibly U show up as thin lines on the maps along the bottom boundary of the titanite. In this position, it is not clear whether these higher concentrations correspond to (i) a concentration of elements within an outer zone of the titanite, or (ii) a concentration of these elements adhering to the mineral's surface. In the adjacent quartz, the fractures appear as thin irregular lines where high X-ray intensities for Fe and, possibly, Zn are observed. In the section shown, these fractures propagate through the quartz and are connected to the grain boundary between the titanite and quartz.

The X-ray maps and BSE images were used to locate the line-scans shown in Figure 1. One line-scan was located across the titanite grain (LS1), and another in the quartz beside the titanite grain (LS2). Figure 3 shows line-scan LS1, which includes contacts with quartz on either side. The horizontal scale is $90\ \mu\text{m}$; the position of the titanite on the scan is shown by the high intensities of Fe, Y, Sr and Nd X-rays. Ca and Ti were not included in these maps, as major-element X-rays would have flooded the detector. Ca and Ti were filtered out by an absorber comprising $106\ \mu\text{m}$ of Al and $125\ \mu\text{m}$ of mylar. The line-scans show elevated concentrations of Fe, Zn, Sr, Y, Pb, and U at the edges of the grain. These elements are also present in the interior of the grain, such that it is still not possible to decide whether the increased concentrations correspond (i) to material adhering to the outside of the

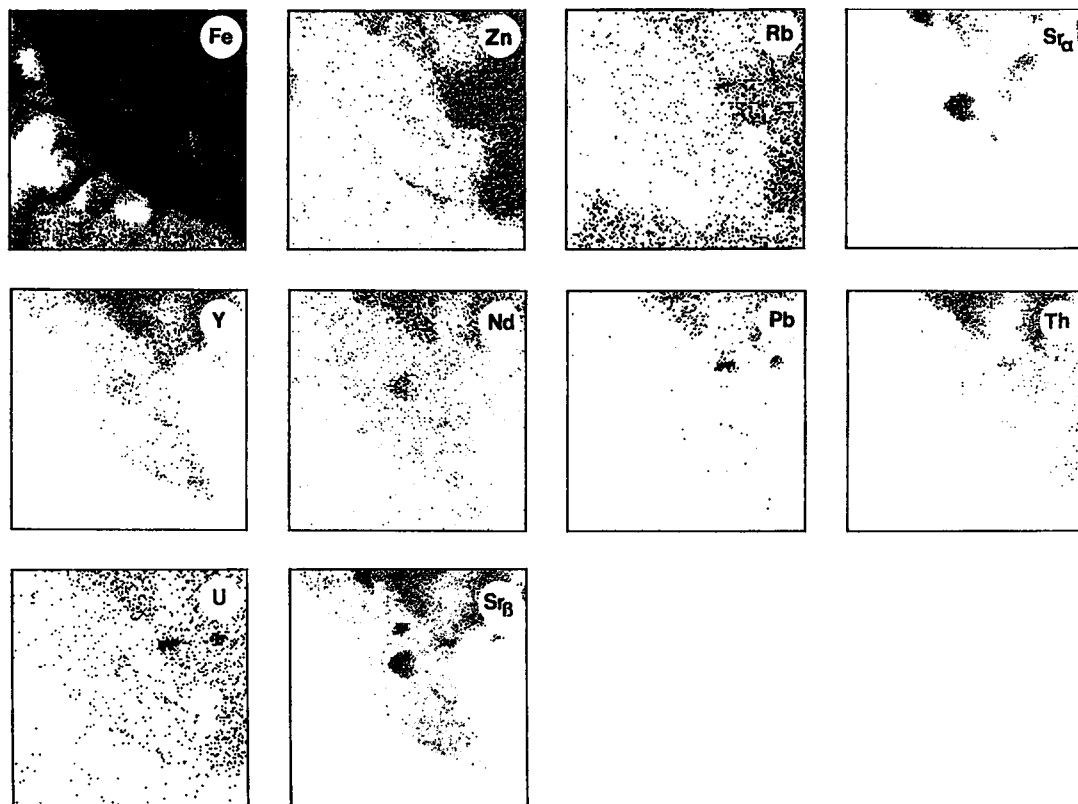


FIG. 2. SPM X-ray map of the titanite grain and surrounding minerals from Figure 1. The distribution of Fe, Zn, Sr, Rb and Y was mapped using *K* X-rays, and that of Nd, Pb, Th and U was mapped using *L* X-rays. A $SrK\beta$ map is included to check its correspondence with the $SrK\alpha$ map. This indicates that the $SrK\alpha$ map is not affected by Fe pile-up.

TABLE 1. X-RAY LINES USED FOR SPM MAPPING AND LINE SCANS

X-ray Line	Window width ¹	Possible interferences related to major elements
FeK α 6.40 keV	0.1 (15 eV)	None
ZnK α 8.63 keV	1.0 (150 eV)	None
RbK α 13.39 keV	0.3 (50 eV)	FeK α + K β pile up 13.45 keV
SrK α 14.16 keV	0.1 (20 eV)	FeK β + K β pile up 14.11 keV
YK α 14.95 keV	0.5 (90 eV)	None
NdL α 5.23 keV	0.2 (30 eV)	FeK β Si escape 5.32 keV
PbL α 10.54 keV	0.5 (80 eV)	None
ThL α 12.96 keV	0.5 (80 eV)	FeK β + K β pile up 12.80 keV
UL α 13.61 keV	0.3 (60 eV)	FeK α + K β pile up 13.45 keV
SrK β 15-16.59 keV ²		None

¹ Mapping window is normally 1 x FWHM of the X-ray line. Factors used to reduce the windows (and hence the possibility of overlap from neighboring lines) are shown. The approximate width of the windows in eV also are shown.

² The SrK β window was set to take in the full width of the SrK β X-ray line.

grain, or (ii) to concentrations of incompatible elements in an outer zone of the titanite. In the case of U, it might be anticipated that Fe pile-up and RbK α X-rays would overlap the UL α X-ray line. The window used to map the distribution of U was restricted to $0.3 \times$ FWHM (60 eV). The distribution of U in the lines-scans differs in detail from that of Rb and Fe with respect to location and relative abundance; this would not be the case if there were significant overlap. With regard to the fractures, the elevated concentrations of U are confirmed by point analyses (see later, Table 2).

Figure 4 shows line-scan LS2 taken within the quartz grain to the lower left of the titanite grain in Figure 1. LS2 crosses a series of fractures within the quartz emanating from the contact with the titanite grain. On the line-scan, the fractures show up by having very high concentrations of Fe, Zn, Rb, Sr, Y, Nd, Pb, U and, possibly, Th. Again, the horizontal distribution of U, Pb and Th differs in detail from that of Fe and Rb. Between, and to either side of the

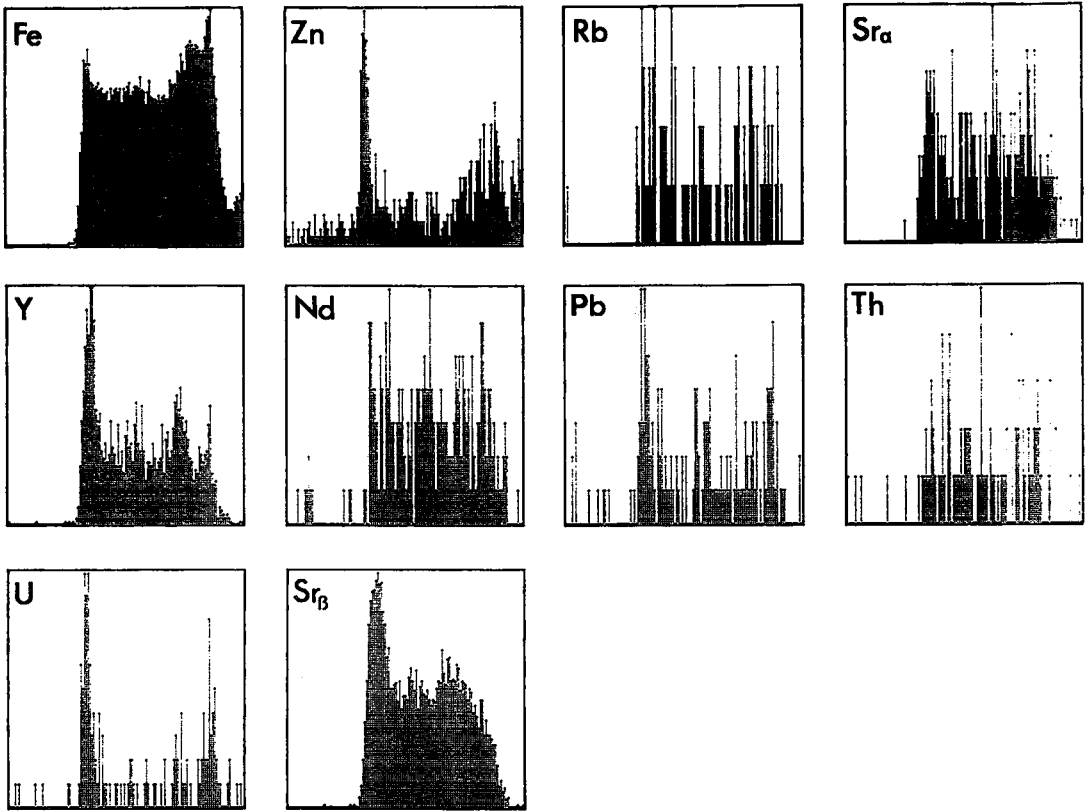


FIG. 3. Line-scan LS1 showing the distribution of trace and minor elements across the titanite grain in Figure 1. Elevated X-ray intensities for Fe, Sr, Y and Nd show the position of the titanite on the scan. Zn, Y and U seem to be concentrated in an outermost zone in the titanite or on the mineral's surface. The $SrK\alpha$ and $SrK\beta$ X-ray maps indicate that the pile up of Fe $K\beta$ + $K\beta$ is not a problem. A comparison of the Fe and U scans show that the Fe peak on the right-hand side of the titanite is larger than that on the left, opposite to what is seen in the distribution of U. This would indicate that Fe $K\alpha$ + $K\beta$ pile up has not been a problem with the restricted U window.

fractures, there are virtually no trace elements present, as would be expected in undamaged quartz. Considering the similarity between the group of elements found in the fractures and grain boundaries, it is likely that their deposition occurred *after* crystallization of the minerals. If the fractures in the quartz were produced during volume changes connected with the metamictization of the britholite, then the britholite could also have been the source of the trace elements. Back-scattered electron images and qualitative energy-dispersion spectra (EDS) of the britholite show that irregular regions with bright grey level have higher abundances of rare-earth elements than darker mottled and fractured regions. One interpretation would be that the more strongly metamict, darker regions had lost their trace elements to the surrounding fractures.

Other grain boundaries and fractures in quartz were scanned. In each case, the same trace-element assemblage was recorded. Figure 5 shows an X-ray map of intersecting cleavage planes in K-feldspar

(about 2 cm away from the titanite grain in Figure 1); the K-feldspar is in contact with britholite. Figure 6 shows line-scan LS3 across the cleavages. In the X-ray maps, high concentrations of Fe and Y can be seen to be related to the distribution of (parallel) cleavages and cross-cutting fractures. In the line-scans, high concentrations of Fe, Zn, Y, Rb, Nd, Pb, Th and U are seen in the cleavages. It is anticipated that Sr would be present in significant amounts in the unfractured K-feldspar (564 ppm; Table 1). Higher concentrations of Sr are seen to correspond to the location of the cleavages; this is more evident in the $SrK\beta$ line-scan.

Point analyses

The line-scans and X-ray maps of grain boundaries, fractures and cleavages in K-feldspar show that these surfaces characteristically contain elevated concentrations of Fe, Zn, Sr, Y, Rb, Nd, Pb, U and, possibly, Th. Along with the X-ray maps, the line-scans also provide

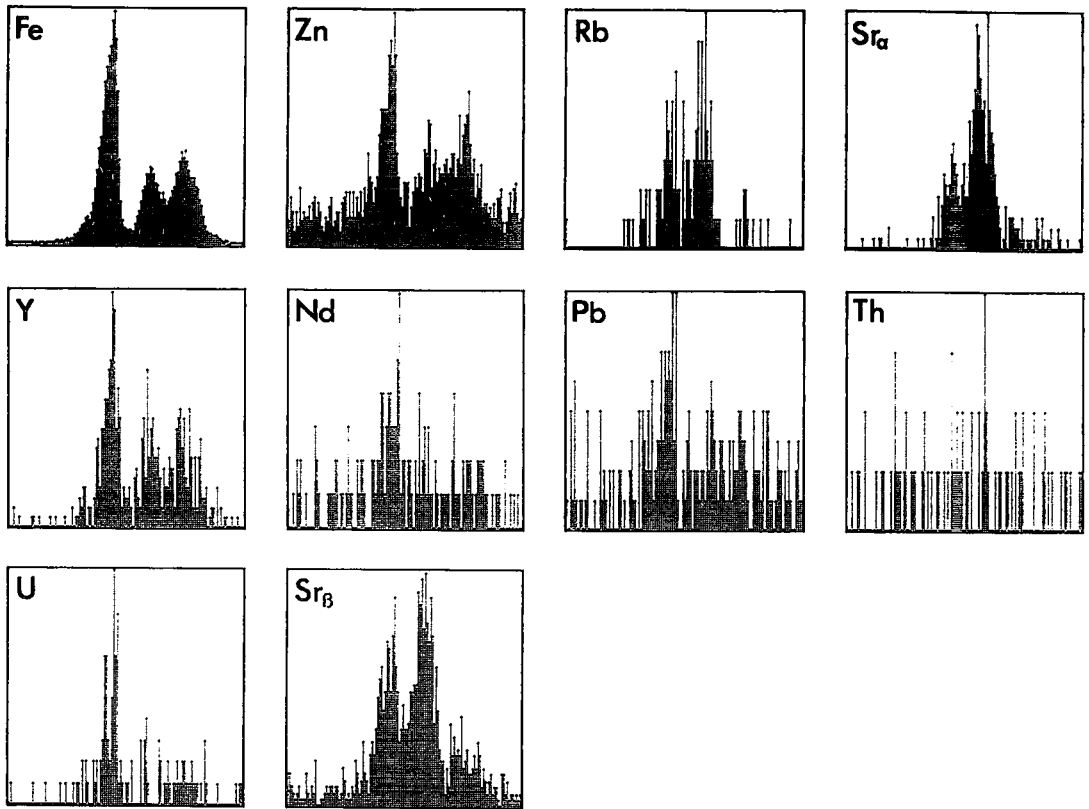


FIG. 4. Line-scan LS2 showing the distribution of trace elements in fractures in quartz. Three fractures were crossed in the line scan; variations in the X-ray intensities suggest that there were probably differences in the abundance of trace elements in the fractures. Comparison of the Sr, Fe and U maps suggests that Fe pile up has not overlapped the Sr and U windows. RbK α X-ray overlap in the U window is not significant.

a good qualitative means of assessing the distribution of these trace elements. Quantitative analysis of these areas is more difficult. Normally, the volume within which proton excitation occurs during analysis can be considered to be a cylinder about 5 μm in diameter by about 20 μm long (the latter dimension depends on the X-ray absorbing power of the matrix). If an analysis of the grain boundary between titanite and quartz were attempted, the proportion of each mineral sampled in this volume (particularly in the case where the contact dips into the section) would be unknown. In such circumstances, it is not possible to carry out matrix corrections on concentrations of trace elements with any confidence.

Where the matrix surrounding the feature of interest consists *only* of one mineral, in this case quartz or feldspar, semiquantitative analyses may be done with more confidence. The volume sampled by the proton beam can be assumed to be stoichiometrically homogeneous in terms of major elements; Si and O in the

case of quartz, and K, Al, Si and O in the case of the K-feldspar. However, the customary quantitative analysis by PIXE assumes that trace elements are homogeneously distributed within a known (or predetermined) matrix; although the trace elements occur on distinct surfaces, their distribution could still be heterogeneous within the $5 \times 5 \times 20 \mu\text{m}$ volume sampled by the proton beam. It is possible that the trace elements may have diffused into structurally disordered regions on either side of the fractures. Even so, it must be stressed that the deduction of elemental concentrations by the usual formalism provides an "order-of-magnitude" estimate, whose main value is an indication of the relative concentrations of the elements concerned.

Figure 7 shows a spectrum collected during analysis of a fracture in quartz from along LS2; for comparison, the inset shows a spectrum collected from a region between the fractures. The "fracture" spectrum shows the K X-rays of Fe, Mn, Zn, Sr, Y, Cu and Zn, and the

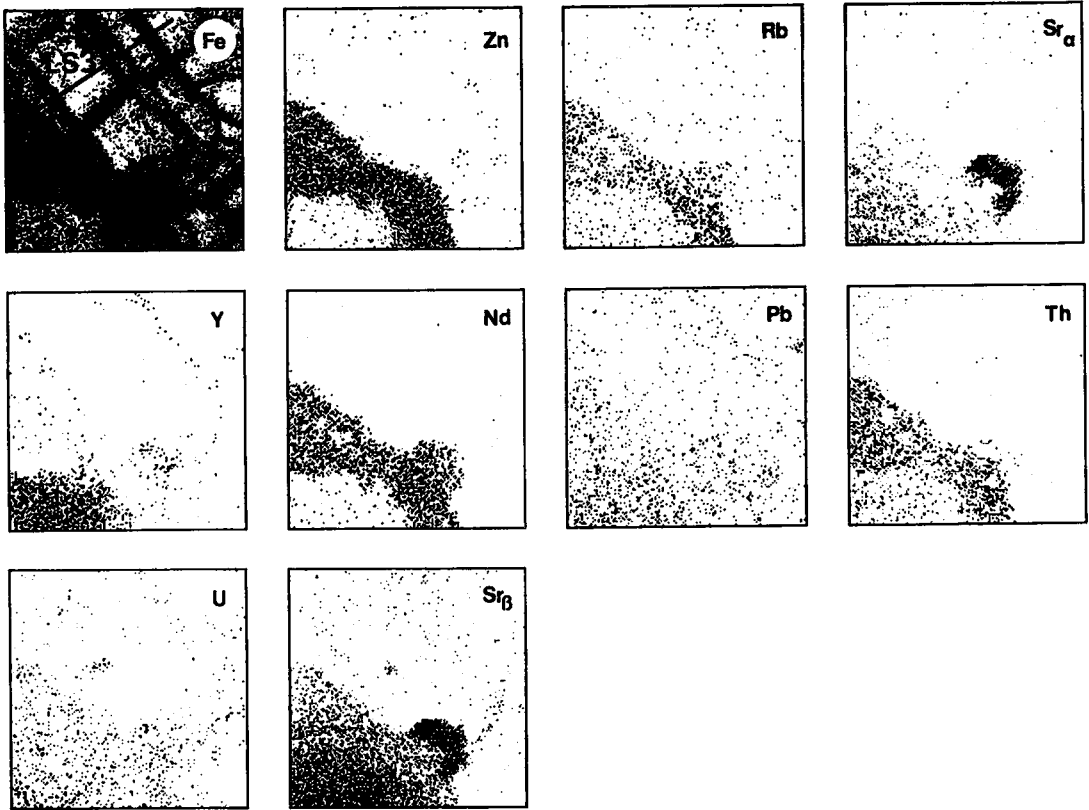


FIG. 5. SPM X-ray map of cleavage planes in K-feldspar adjacent to metamict britholite (seen as the black region on the Fe, Zn and Nd maps). The position of line-scan LS3 (Fig. 6) is shown on the Fe map.

L X-rays of Ce, Nd, Pb and U, whereas the spectrum from the quartz is virtually featureless. Table 2 shows trace-element data from analyses of quartz fractures, quartz, K-feldspar cleavages and K-feldspar. Both the fractures in quartz and the cleavages in feldspar show significant concentrations of trace elements, higher than is observed in unfractured quartz and unaltered feldspar between the cleavages. During normal igneous crystallization, trace quantities of Rb, Th, U, Sr and Pb may be incorporated in feldspars; the elevated concentration of these elements along cleavages suggests that they have been introduced to these areas after formation of the mineral.

DISCUSSION

From a physical point of view, the three types of surface discussed are different; the orientation and connectivity of grain boundaries will be determined by grain size and shape, and as such could be considered

TABLE 2. ELEMENT CONCENTRATIONS (PPM) IN QUARTZ (Q), QUARTZ FRACTURES (QF), FELDSPAR CLEAVAGE (FC) AND FELDSPAR (F)

	QF1	QF2	Q1	Q2	FC	F	LOD ²
Mn	226 (9) ¹	70 (5)	—	—	327 (15)	—	1-9
Fe	4352 (7)	1654 (5)	23	39	4778 (12)	220 (4)	1-13
Zn	27 (1)	10 (1)	—	—	15 (1)	—	0.5-1
Ga	—	—	—	—	13 (1)	15 (1)	1
Rb	13 (1)	—	—	—	4 (1)	—	1-2
Sr	104 (2)	217 (2)	—	—	790 (4)	564 (4)	1-1.5
Y	114 (2)	27 (1)	—	—	132 (2)	3 (1)	1-2
Nd	250 (32)	406 (39)	—	—	736 (67)	—	67-143
Bu	—	—	—	—	220 (43)	—	110
Pb	26 (1)	8 (1)	—	—	55 (2)	—	2-3
Th	—	—	—	—	31 (3)	18 (2)	3-6
U	73 (3)	8 (2)	—	—	71 (4)	—	3-7

¹ numbers in parentheses represent 1 σ statistical error (ppm) of the spectrum fitting procedure
² LOD, lower limit of detection (ppm), LODs for the individual analyses span the given range.

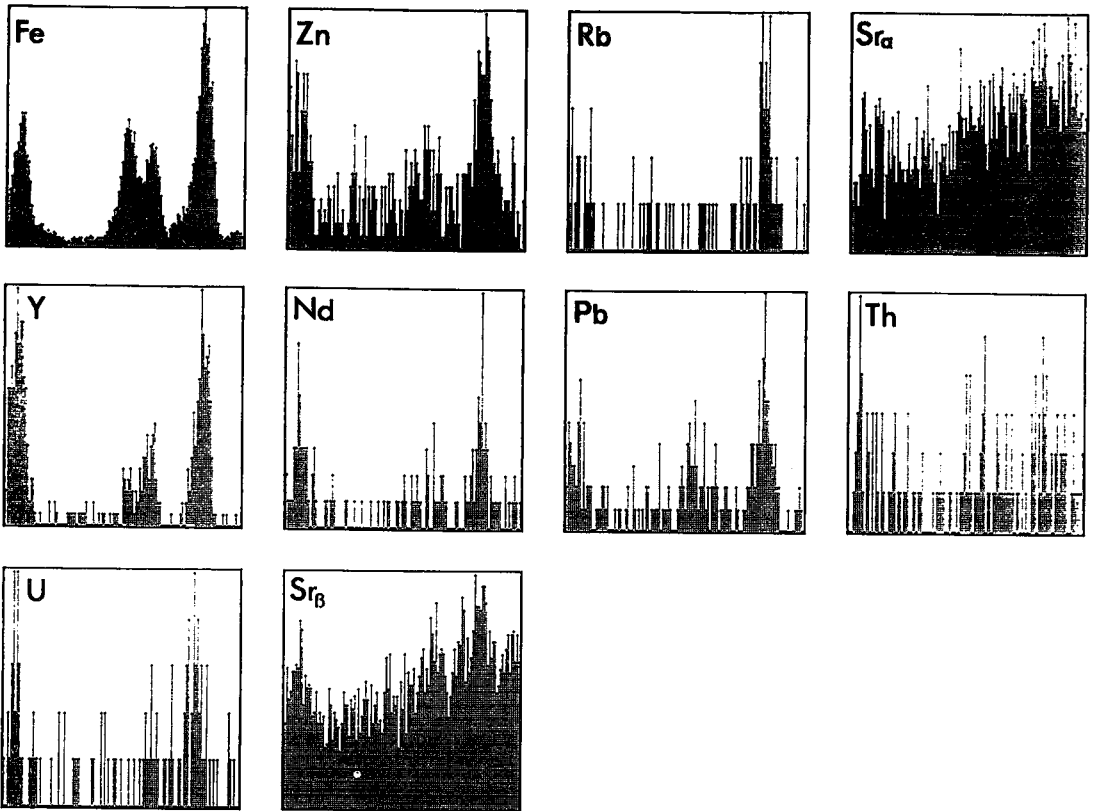


FIG. 6. Line-scan LS3 showing the distribution of trace elements in K-feldspar cleavage planes. Fe, Zn, Y, Nd, Pb and U show a similar pattern of distribution; Th is close to its detection limits. Sr shows up throughout the scan as it is a trace component in the feldspar, but it shows elevated abundance along two of the cleavages.

as intrinsic features of the rock texture. From a chemical perspective, grain boundaries offer a chemically reactive environment for the deposition or attachment of ions or ionic complexes. Cleavages in a mineral reflect the internal arrangement of atoms and chemical composition of that mineral, and can be considered an intrinsic feature of the mineral, but could still offer different structural and chemical environments for reactions. The fractures that cross-cut minerals, such as quartz, are stress-induced features that postdate the formation of the mineral. The analytical problems that such surfaces present may be overcome; it should not be difficult to extend the model used for X-ray production (Maxwell *et al.* 1989) to deal with a localized "sheet" of elements adhering to a surface. This would provide a more realistic estimate of the concentrations of the various trace elements concerned.

The concentration and similarity of the suite of trace elements along the fractures in quartz, grain boundaries

and feldspar cleavages are consistent with deposition from a fluid that had moved along these surfaces after the crystallization of the rock; the similarity in the element assemblage also suggests that the surfaces were connected. Slight differences in composition could be attributed to differences in the local environment determined by the nature of the surrounding minerals.

The mobility of *REE* and *HFSE* in an aqueous solution is enhanced by the presence and concentration of F^- , Cl^- , SO_4^{2-} and CO_3^{2-} . Fluorite and wloganite are present in the rock [whole-rock F contents range from 200 to 4000 ppm (Halden & Fryer, unpubl. data)], so that F^- and CO_3^{2-} were probably present in an altering fluid. These ions and complexes are expected to increase the solubility of the *REE*. The presence of fluorine could also have contributed to the instability of the britholite. Other factors affecting the mobility of the *REE* include the pH of the coexisting aqueous solution; Humphris (1984) pointed out that *REE* can

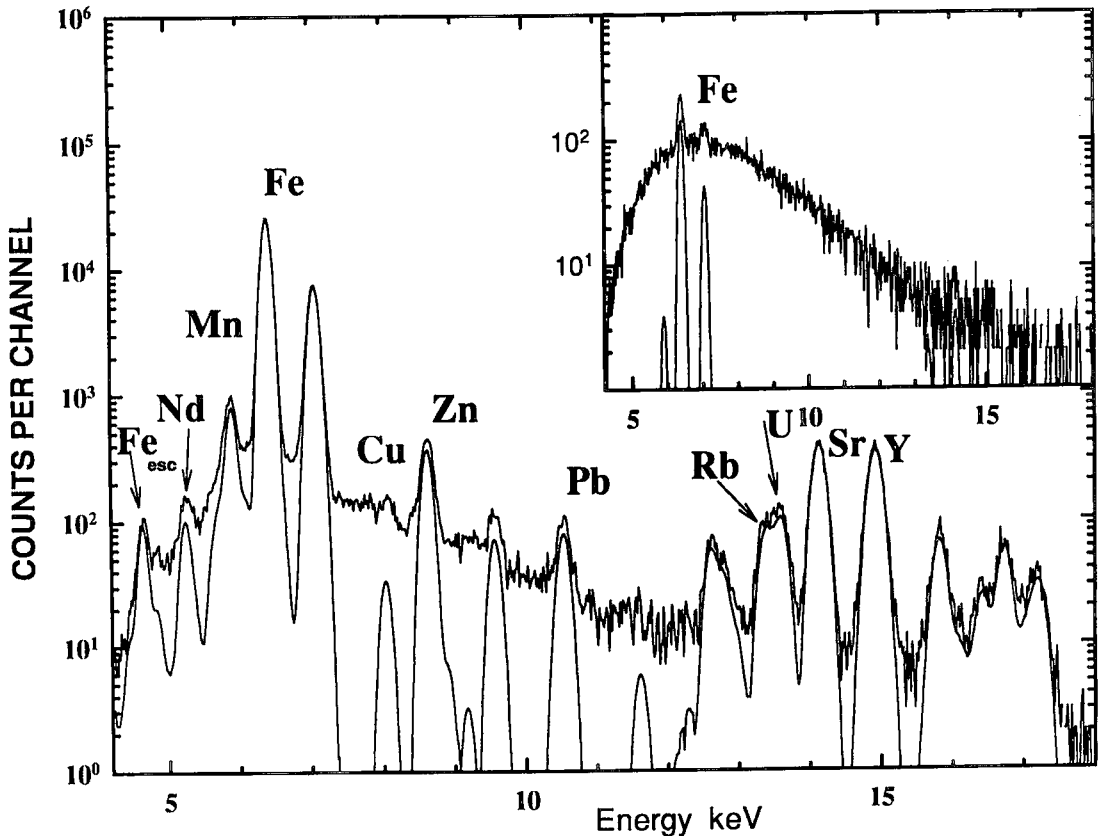


FIG. 7. PIXE spectrum from a fracture in quartz showing the K X-rays of Mn, Fe, Cu, Zn, Rb, Sr and Y, and L X-rays of Nd, Pb and U (only the main X-ray peaks are labeled; Fe_{esc} refers to the Fe escape peak). The inset spectrum shows a PIXE spectrum taken from between fractures in undamaged quartz; it only shows Fe X-ray peaks.

be removed from regions of a rock that has been weathered by acidic solutions and subsequently re-deposited (adsorbed) in areas where the pH increased. The proximity of the metamict britholite to the regions mapped make it the most likely source of the trace and minor elements. However, contributions coming from other minerals cannot be excluded; decomposition of the titanite (although there is no obvious visible evidence) could have contributed Y, Zr, Ti, REE and Fe to coexisting aqueous solutions (*cf.* Bancroft *et al.* 1987, Pan *et al.* 1993).

In the Eden Lake syenite, britholite occurs in the cross-cutting pegmatites as irregular segregations that have embayed contacts with the principal silicate minerals. The irregular form of the contact suggests that the britholite may have been formed by the injection of a phosphorus-rich REE-bearing fluid that reacted with the silicate minerals. On the basis of the distribution of the minor and trace elements alone, it is not possible to determine the P-T conditions for this

reaction. However, Lira & Ripley (1992) suggested that the occurrence of britholite in the Rodeo de Los Molles deposit, central Argentina, was the product of hydrothermal alteration at temperatures less than 350°C (based on fluid-inclusion studies). This inference is not inconsistent with the temperatures of alteration proposed for the Zr-, Y-, REE-bearing Strange Lake deposit (Salvi & Williams-Jones 1990). The presence of weloganite in the titanite could also be interpreted as being related to alteration; Schuling & Vink (1967) showed that equilibrium curve for the reaction titanite + $CO_2 \rightleftharpoons$ anatase + calcite + quartz lies between 340 and 450°C. Although ongoing studies show that there are small amounts of REE-bearing carbonates associated with the accessory minerals, most of these occur as inclusions, which would suggest that these were the product of early crystallization, not alteration.

In this study, the (inferred) altering fluid is no longer available for analysis; however, it has left a record of

its passage by depositing trace elements along the path of its migration. The mineralogical nature of what was deposited is not clear. The chemical makeup of a coexisting fluid is likely to have included other ions such as Fe^{2+} , Mg^{2+} , Na^+ , K^+ and $\text{H}_2\text{SiO}_4^{2-}$ coming from the decomposition of feldspars and aegirine-augite. If these ions were present, minerals such as chrysotile could have been deposited along the grain boundaries and fractures. In the case of the K-feldspar cleavages, *in situ* alteration to clay minerals (such kaolinite and illite) may have provided sites on which trace elements could be adsorbed.

Other problems connected with minor- and trace-element mobility

The probability that elements such as Th, U and Pb can be mobile, particularly in the vicinity of a metamict mineral such as britholite, could have implications for the disposal of radioactive wastes. Primary porosity and permeability are usually very low in igneous rocks, making bulk migration of fluid very slow; significant migration of fluid in such rocks is usually restricted to secondary porosity (faults, joints, *etc.*). The primary porosity of an igneous rock will include any space related to small-scale planar features such as grain boundaries, mineral cleavages and fractures; for a fluid to flow, these features must be connected.

Many granite batholiths (a currently favored buffer-formation as a site for the disposal of radioactive wastes) contain radioactive minerals, for example allanite and zircon. Both allanite and zircon can become metamict with time and undergo a change in volume. Such changes in volume can exert stresses on the surrounding minerals, resulting in fracturing, which could impart a type of secondary porosity to the rock. Another way of increasing the surface area available for fluid migration (and for chemical reaction) is the release of the confining pressure on the rocks, such as might occur during the construction (or mining) of a disposal vault; here the grain boundaries could provide secondary pathways for element migration. Pan *et al.* (1993) suggested that intergranular diffusion along grain boundaries and planar defects is the process whereby elements migrate during the breakdown of minerals such as titanite.

In this study, we have shown that grain boundaries, cleavages and fractures can contain significant concentrations of trace elements and might also act as conduits for the transport and deposition of trace elements. Metamict minerals could contribute some of the trace element make-up of a migrating fluid; however, if the primary buffer in a disposal vault were to fail, radioactive waste also could migrate. The intrinsic mineralogical characteristics of the buffer rock are important factors in estimating the porosity and permeability (and the background chemical) characteristics of the rock. Where it is necessary to

understand the distribution of trace elements within these buffers, PIXE and SPM can provide valuable information concerning the sites and levels of concentration of the trace elements.

Petrogenetic implications of rare-element mobility

The distribution of trace elements within and between minerals is at the root of most geochemical methods of tectonic discrimination. The *REE*, *LIL* and *HFS* elements are normally considered to be immobile. Goni (1966) provided some early evidence regarding the distribution and mobility of trace elements, so we really should not be surprised that trace elements are commonly not "as well behaved" as we might like. This is normally attributed to *anomalous* behavior of trace elements or to contamination of the whole rock's composition without further elaboration. Typically, our response to this has been to develop models of increasing complexity to explain *anomalous* distribution and concentrations of trace elements. An alternative would be to recognize that with new analytical techniques, we can assess the spatial distribution of trace elements as well as their concentration.

If mineral surfaces can preferentially concentrate certain elements, bulk-rock data will not reflect the concentration of trace elements in the minerals of the rock; traditional methods of mineral analysis either remove, or avoid analysis of, mineral surfaces. Bulk-rock chemical data include contributions by elements adhering to mineral surfaces; therefore, petrogenetic models based on bulk-rock chemistry are likely to include significant scatter. *Trace-element* micro-analytical techniques are necessary to correct this problem and to check the correspondence of mineral chemistry to whole-rock chemistry. In this work, SPM and μ -PIXE are shown to be effective tools in mapping the distribution of trace elements along mineral boundaries, cleavages and fractures, and for the analysis of the host minerals.

ACKNOWLEDGEMENTS

This work was supported by NSERC and LITHO-PROBE grants to NMH, and NSERC grants to JLC. We thank R.F. Martin, Timo Nijland, Dick Lieftink, B. Bonin and anonymous reviewers for their constructive criticism of an earlier version of the manuscript.

REFERENCES

- ANDERSON, A.J., CLARK, A.H., MA, XIN-PEI, PALMER, G.R., MACARTHUR, J.D. & ROEDER, E. (1989): Proton-induced X-ray and gamma ray emission analysis of unopened fluid inclusions. *Econ. Geol.* **84**, 924-939.

- BANCROFT, G.M., METSON, J.B., KRESOVIC, R.A. & NESBITT, H.W. (1987): Leaching studies of natural and synthetic titanites using secondary ion mass spectrometry. *Geochim. Cosmochim. Acta* **51**, 911-918.
- FRASER, D.G., WATT, F., GRIME, G.W. & TAKACS, J. (1984): Direct determination of strontium enrichment on grain boundaries in a garnet ilmenite xenolith by proton microprobe analysis. *Nature* **312**, 352-354.
- GONI, J. (1966): Contribution à l'étude de la localisation et de la distribution des éléments en traces dans les minéraux et les roches granitiques. *Bureau de Recherches Géol. Minières, Mém.* **45**.
- GREEN, T.H., SIE, S.H., RYAN, C.G. & COUSENS, D.R. (1989): Proton microprobe-determined partitioning of Nb, Ta, Zr, Sr, and Y between garnet, clinopyroxene and basaltic magma at high pressure and temperature. *Chem. Geol.* **74**, 201-216.
- HALDEN, N.M., HAWTHORNE, F.C., CAMPBELL, J.L., TEESDALE, W.J., MAXWELL, J. & HIGUCHI, D. (1993): Chemical characterization of oscillatory zoning and overgrowths in zircon using 3 MeV μ -PIXE. *Can. Mineral.* **31**, 637-647.
- HOCHHELLA, M.F., JR. & WHITE, A.F. (1990): Mineral-water interface geochemistry. In *Mineral-Water Interface Geochemistry* (M.F. Hochella, Jr. & A.F. White, eds.). *Rev. Mineral.* **23**, 1-16.
- HUMPHRIS, S. (1984): The mobility of rare earth elements in the crust. In *Rare Earth Element Geochemistry* (P. Henderson, ed.). Elsevier, Amsterdam, The Netherlands (317-342).
- JACKSON, S.E., LONGERICH, H.P., DUNNING, G.R. & FRYER, B.J. (1992): The application of laser ablation microprobe - inductively coupled plasma - mass spectrometry (LAM-ICP-MS) to in situ trace-element determinations in minerals. *Can. Mineral.* **30**, 1049-1064.
- LIRA, R. & RIPLEY, E.M. (1992): Hydrothermal alteration and REE-Th mineralization at the Rodeo de Los Molles deposit, Las Chacras batholith, central Argentina. *Contrib. Mineral. Petrol.* **110**, 370-386.
- MAXWELL, J.L., CAMPBELL, J.L. & TEESDALE, W.J. (1989): The Guelph PIXE software package. *Nucl. Instrum. Methods Phys. Res.* **B43**, 218-230.
- MCRITCHIE, W.D. (1988): Alkaline intrusions of the Churchill Province: Eden Lake (64C/9). In *Manitoba Energy and Mines, Minerals Div., Rep. Field Activities* 1988, 5-11.
- _____ (1989): Ground scintillometer reconnaissance of the Eden Lake aegirine-augite monzonite. In *Manitoba Energy and Mines, Minerals Div., Rep. Field Activities* 1989, 7-12.
- O'REILLY, S.Y., GRIFFIN, W.L. & RYAN, C.G. (1991): Residence of trace elements in metasomatized spinel ilmenite xenoliths: a proton microprobe study. *Contrib. Mineral. Petrol.* **109**, 98-113.
- PAN, YUANMING, FLEET, M.E. & MACRAE, N.D. (1993): Late alteration in titanite (CaTiSiO₅): redistribution and remobilization of rare earth elements and implications for U/Pb and Th/Pb geochronology and nuclear waste disposal. *Geochim. Cosmochim. Acta* **57**, 355-367.
- SALVI, S. & WILLIAMS-JONES, A.E. (1990): The role of hydrothermal processes in the granite hosted Zr, Y, REE deposit at Strange Lake, Quebec/Labrador: evidence from fluid inclusions. *Geochim. Cosmochim. Acta* **54**, 2403-2418.
- SCHULING, R.D. & VINK, B.W. (1967): Stability relations of some titanium-minerals (sphene, perovskite, rutile, anatase). *Geochim. Cosmochim. Acta* **31**, 2399-2411.
- TEESDALE, W.J., CAMPBELL, J.L. & HALDEN, N.M. (1993): Two-dimensional mapping of element variation in minerals using the Guelph Proton Microprobe. *Nucl. Instrum. Methods Phys. Res.* **B77**, 405-409.

Received April 23, 1993, revised manuscript accepted March 26, 1995.